Available online at www.sciencedirect.com
SCIENCE DIRECT®
Analytica Chimica Acta 541 (2005) 143–150
ANALYTICA CHIMICA ACTA
www.elsevier.com/locate/aca

Electrogenerated chemiluminescence (ECL) 79. Reductive-oxidation ECL of tris(2,2′-bipyridine)ruthenium(II) using hydrogen peroxide as a coreactant in pH 7.5 phosphate buffer solution

Jai-Pil Choi[1], Allen J. Bard*

Department of Chemistry and Biochemistry, The University of Texas at Austin, 1 University Station, Austin, TX 78712, USA

Received 1 July 2004; received in revised form 29 November 2004; accepted 29 November 2004
Available online 5 January 2005

Abstract

Hydrogen peroxide (H_2O_2) can be used as a coreactant to generate reductive-oxidation ECL of Tris(2,2′-bipyridine)ruthenium(II), $Ru(bpy)_3^{2+}$ (bpy = 2,2′-bipyridine), in pH 7.5 phosphate buffer solution (PBS). Although $Ru(bpy)_3^{+}$ is adsorbed and precipitated on the electrode upon reduction of $Ru(bpy)_3^{2+}$ in aqueous solutions, ECL can still be generated and scanning electrochemical microscopy (SECM) experiments verified the presence of some dissolved $Ru(bpy)_3^{+}$ in the solution. When H_2O_2 is electrochemically reduced, it produces hydroxyl radical ($^{\bullet}OH$). ECL is generated by an energetic electron transfer (ET) reaction between $Ru(bpy)_3^{+}$ and $^{\bullet}OH$. The ECL intensity depends on both the $Ru(bpy)_3^{2+}$ and H_2O_2 concentrations. However, a relatively high concentration of H_2O_2 (>1 mM H_2O_2 with 0.1 mM $Ru(bpy)_3^{2+}$) quenches ECL significantly. H_2O_2 also quenches the photoluminescence of $Ru(bpy)_3^{2+}$ with a quenching rate constant of $5.7 \times 10^6\ M^{-1}\ s^{-1}$.

Keywords: Tris(2,2′-bipyridine)ruthenium(II); Hydrogen peroxide; Electrogenerated chemiluminescence (ECL); Coreactant; Hydroxyl radical; Quencher

1. Introduction

Electrogenerated chemiluminescence (ECL) involves light emission that arises from a highly energetic electron transfer (ET) reaction between electrogenerated species. Usually, the emitting species is regenerated after ECL [1–3]. There are two main methods of generating ECL. The first is ion annihilation, which involves ET between oppositely charged radical ions ($R^{\bullet -}$ and $R^{\bullet +}$) generated at an electrode (vide infra):

$$R^{\bullet -} + R^{\bullet +} \rightarrow R + R^{*} \quad (1)$$

$$R^{*} \rightarrow R + h\nu \quad (2)$$

where R is an ECL emitter.

The second involves the use of a coreactant, that produces a strong reducing or oxidizing agent in a reaction following ET. Employing a coreactant is useful especially when either $R^{\bullet +}$ or $R^{\bullet -}$ is not sufficiently stable for the ECL annihilation reaction, or when the solvent has a narrow potential window so that $R^{\bullet +}$ and $R^{\bullet -}$ cannot both be formed. With a coreactant, ECL can be generated by applying a potential in one direction. Depending on the reaction path to produce the ECL emitter in the excited state, it is referred to as oxidative-reduction or reductive-oxidation ECL. For example, oxalate ion (C_2O_4) [4,5] and various amines [6–9] are used for oxidative-reduction ECL where an oxidative step produces a strong reductant. Peroxidisulfate ion ($S_2O_8^{2-}$) [10–12] is frequently used for reductive-oxidation ECL. A widely used system for coreactant ECL is the $Ru(bpy)_3^{2+}$/tri-*n*-propylamine (TPrA) system [8,13], shown below:

$$Pr_2N{-}CH_2{-}Et - e^{-} \rightarrow Pr_2N^{\bullet +}{-}CH_2{-}Et \quad (3)$$

$$Pr_2N^{\bullet +}{-}CH_2{-}Et \rightarrow Pr_2N{-}C^{\bullet}H{-}Et \quad (4)$$

* Corresponding author. Tel.: +1 512 471 3761; fax: +1 512 471 0088.
E-mail address: ajbard@mail.utexas.edu (A.J. Bard).
[1] Present address: Kenan Laboratories of Chemistry, University of North Carolina, Chapel Hill, NC 27599-3290, USA.

0003-2670/$ – see front matter © 2004 Elsevier B.V. All rights reserved.
doi:10.1016/j.aca.2004.11.075

$$Ru(bpy)_3^{2+} - e^- \rightarrow Ru(bpy)_3^{3+} \quad (5)$$

$$Ru(bpy)_3^{3+} + Pr_2N{-}C^{\bullet}H{-}Et \rightarrow Ru(bpy)_3^{2+*} + P \quad (6)$$

or

$$Ru(bpy)_3^{2+} + Pr_2N{-}C^{\bullet}H{-}Et \rightarrow Ru(bpy)_3^{+} + P \quad (7)$$

$$Ru(bpy)_3^{3+}\ (\text{from Eq. (5)}) + Ru(bpy)_3^{+} \rightarrow Ru(bpy)_3^{2+*} + Ru(bpy)_3^{2+} \quad (8)$$

where Pr is $CH_3CH_2CH_2-$, Et is CH_3CH_2-, and P is a reaction product.

ECL produced by a coreactant has been used in a variety of aqueous analytical techniques [2,14–17], because the electrochemical potential window of an aqueous solution is too narrow to readily produce both sufficiently stable radical cations and anions for annihilation ECL. Therefore, development of a coreactant is important in adopting ECL in such analytical techniques as well as improving sensitivity and reproducibility of the ECL emitter/coreactant system.

H_2O_2 as a coreactant in ECL has not yet been reported. In this paper, we demonstrate that hydrogen peroxide (H_2O_2) can be used as a coreactant to generate ECL of $Ru(bpy)_3^{2+}$ in an aqueous solution via reductive-oxidation. We also discuss electrochemical reduction of $Ru(bpy)_3^{2+}$ in pH 7.5 phosphate buffer solution (PBS) using cyclic voltammetry and scanning electrochemical microscopy (SECM).

2. Experimental

2.1. Chemicals and solutions

Tris(2,2′-bipyridine)dichlororuthenium(II) hexahydrate, $Ru(bpy)_3Cl_2{\cdot}6H_2O$ (99.99%) and sodium hydroxide were obtained from Aldrich (Milwaukee, WI) and used as received. Hydrogen peroxide (30%), $NaH_2PO_4{\cdot}H_2O$, and $Na_2HPO_4{\cdot}12H_2O$ from Fischer Scientific Co. (Fair Lawn, NJ) were used without further purification. Phosphate buffer solution (PBS) (0.2 M) was prepared by a literature method [18] and the pH was adjusted to 7.5 by addition of 2 M NaOH. All aqueous solutions used in this work were prepared with deionized water (MilliQ, Millipore).

2.2. Electrochemistry

A conventional three-electrode electrochemical cell was used for the electrochemistry and ECL experiments. Glassy carbon (GCE, 0.07 cm^2), platinum wire (Pt, 0.4 mm diameter), and silver/silver chloride (Ag/AgCl in saturated potassium chloride solution) were employed as working, counter (or auxiliary), and reference electrodes, respectively. Cyclic voltammograms (CVs) were obtained with either a CHI 660 electrochemical workstation (CH Instruments, Austin, TX) or a homemade potentiostat. All potentials are reported in V versus Ag/AgCl, unless mentioned otherwise. All solutions used for electrochemistry and ECL were purged with nitrogen gas to remove oxygen, unless mentioned otherwise.

2.3. Scanning electrochemical microscopy (SECM)

SECM measurements were performed with a CHI-900 scanning electrochemical microscope (CH Instruments, Austin, TX). An annealed carbon fiber 10 μm diameter (Goodfellow, Cambridge, UK) was heat-sealed in a glass capillary to prepare the SECM tip as described previously [19]. The RG value of this tip was 5, determined from measurements with an optical microscope. A GCE (0.07 cm^2) was used as the substrate electrode. The tip was polished and rinsed with water and acetone prior to each measurement.

2.4. Photoluminescence and ECL measurements

Photoluminescence (PL) spectra were obtained with an ISA Spex Fluorolog-3 (JY Horiba, Edison, NJ). A quartz cuvette with a 1 cm path length was used for all PL measurements. All solutions used for PL were purged with N_2 gas.

To obtain a simultaneous CV and integrated ECL signal, a photomultiplier tube (PMT, Hamamatsu R4220p) was used, with −750 V supplied to the PMT with a high-voltage power supply series 225 (Bertan High Voltage Co., Hicksville, NY). The ECL spectrum was measured as previously reported [20]. A charge-coupled device (CCD) camera (Photometrics CH260, Tucson, AZ) cooled to −110 °C and interfaced to a computer was used to obtain the ECL spectra. The CCD camera was focused on the exit slit of a grating spectrometer (concave grating) having a 1 mm entrance slit (Holographics, Inc.). All integrated ECL signals were produced by scanning potentials from 0 V to a potential sufficiently negative to reduce both H_2O_2 and $Ru(bpy)_3^{2+}$. The ECL spectrum was produced by pulsing the potential from 0 to −1.5 V.

3. Results and discussion

3.1. Electrochemical reduction of $Ru(bpy)_3^{2+}$ in pH 7.5 PBS

Electrochemical reduction of $Ru(bpy)_3^{2+}$ in aqueous solutions is rarely discussed, because the potential window of water is narrow and the background reduction current of water interferes with the reduction waves of $Ru(bpy)_3^{2+}$ in CV. However, one can see a reduction wave of $Ru(bpy)_3^{2+}$ in CV even in the aqueous solution, if the following conditions are satisfied: (a) low proton (H^+) concentration, (b) sufficiently high concentration of $Ru(bpy)_3^{2+}$ to overcome the background reduction current of water, and (c) use of a GCE that has more negative overpotential for H^+ and water reduction than metal electrodes, such as Pt and Au. For example, Fiaccabrino et al. [21] showed that ECL could be

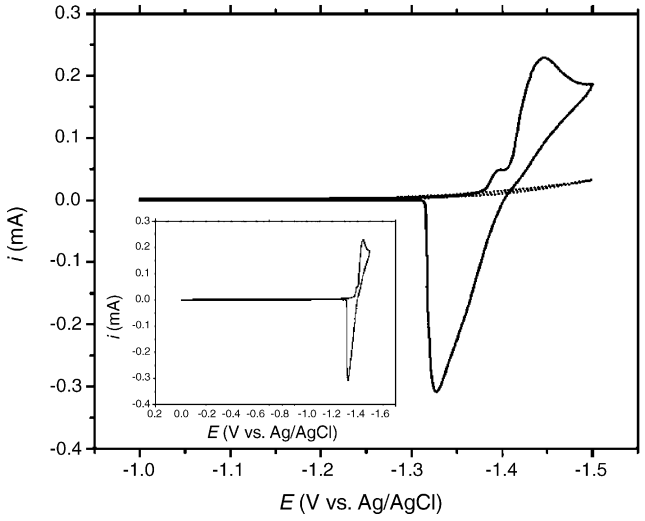

Fig. 1. Cyclic voltammogram (CV) of 5 mM $Ru(bpy)_3^{2+}$ (solid line) in pH 7.5 PBS at 0.1 V/s. The dotted line represents the background CV at 0.1 V/s. Inset is CV of 5 mM $Ru(bpy)_3^{2+}$ under same conditions but scanned from 0.0 V. All CVs were measured at GCE (0.07 cm^2).

obtained with the $Ru(bpy)_3^{2+}$ system in aqueous solution by generation of the +1 and +3 species. They also demonstrated production of dissolved $Ru(bpy)_3^{+}$ in aqueous solution by a generation/collection experiment using carbon interdigitated microelectrode arrays.

Fig. 1 shows CV of 5 mM $Ru(bpy)_3^{2+}$ in pH 7.5 PBS, measured at GCE (0.07 cm^2) with a scan rate of 0.1 V/s. Oxygen was removed from the solution by bubbling N_2 gas for at least 1 min. Although water began to be reduced at around −1.25 V, this background current did not interfere with the first reduction of $Ru(bpy)_3^{2+}$. Unlike the reduction wave of $Ru(bpy)_3^{2+}$ in nonaqueous solvents (e.g., acetonitrile) [22,23], the reduction of $Ru(bpy)_3^{2+}$ in pH 7.5 PBS showed two waves: a small wave at −1.39 V and a larger one at −1.45 V. When the electrode potential scan was reversed at −1.50 V, a large and sharp oxidation peak was observed at −1.33 V.

To analyze these waves, we carried out experiments of the scan rate (ν) dependence of the CV behavior. Fig. 2 shows the CVs of 5 mM $Ru(bpy)_3^{2+}$ in pH 7.5 PBS at various scan rates (0.02–0.5 V/s). In Fig. 2(a), two consecutive waves appeared at all scan rates. As shown in Fig. 2(b) and (c), i_p of the first wave linearly increased with ν (but not with $\nu^{1/2}$) and showed at zero intercept. On the other hand, i_p of the second wave was linearly dependent with zero intercept only with $\nu^{1/2}$. Based on these results, the i_p of the first wave is not diffusion-controlled and the prewave probably results from a product (here $Ru(bpy)_3^{+}$) strongly adsorbing on the electrode [24,25]. This prewave is followed by a diffusion-controlled wave for reduction of dissolved $Ru(bpy)_3^{2+}$ to dissolved $Ru(bpy)_3^{+}$. The prewave exists because the free energy of adsorption of $Ru(bpy)_3^{+}$ makes reduction of $Ru(bpy)_3^{2+}$ to adsorbed $Ru(bpy)_3^{+}$ easier than reduction to $Ru(bpy)_3^{+}$ in solution. In addition, the calculated charge (average, 10.4 ± 0.7 μC) of the prewave was independent of the $Ru(bpy)_3^{2+}$ concentration from 2 to 7 mM. However, when the electrode potential was scanned back, the corresponding diffusion-controlled wave and prewave for oxidation of $Ru(bpy)_3^{+}$ were not observed in the CV (Fig. 2(a)). Instead, a sharp oxidation peak appeared with the characteristic stripping peak shape. This may indicate that some precipitation of $Ru(bpy)_3^{+}$ also occurs on the electrode in addition to adsorption. The solubility of Ru complexes having highly hydrophobic bipyridine ligands probably decreases in the aqueous solution upon reduction of the charge. Similar results were reported for an acetonitrile–water (1:1, v/v) mixture [26].

Even though adsorption and precipitation of $Ru(bpy)_3^{+}$ occurs, some dissolved $Ru(bpy)_3^{+}$ is formed in the aqueous solution. To verify this, tip approach experiments were performed using SECM. The substrate-generation/tip-collection (SG/TC) mode was chosen because the glassy carbon substrate (0.07 cm^2) produced a larger diffusional flux of $Ru(bpy)_3^{+}$ than the carbon fiber tip. Fig. 3 shows the experimental approach curve for reduction of 1 mM $Ru(bpy)_3^{2+}$/pH 7.5 PBS at the substrate held at −1.48 V and the tip at −1.2 V to oxidize $Ru(bpy)_3^{+}$ back to $Ru(bpy)_3^{2+}$. As the tip approached to the substrate (at 2 μm/s), the tip current (i_{tip}) increased because of the concentration gradient of $Ru(bpy)_3^{+}$ produced at the substrate electrode as well as the positive feedback mode of the tip [27]. This indicates that dissolved $Ru(bpy)_3^{+}$ is also generated upon $Ru(bpy)_3^{2+}$ reduction. Once the tip made contact with the substrate, i_{tip} steeply increased and this point was designated as $d = 0$ μm (d is the distance between tip and substrate).

3.2. Electrochemical reduction of hydrogen peroxide (H_2O_2)

Electrochemical reduction of H_2O_2 shows a broad irreversible wave in CV.

Fig. 4 shows CVs of 10 mM H_2O_2 in pH 7.5 PBS measured at various scan rates. H_2O_2 began to reduce at −0.4 V at GCE and peak potentials (E_p) shifted in a negative direction as a function of ν (inset of Fig. 3). Assuming that electrochemical reduction of H_2O_2 is a totally irreversible system with the rate-determining step of the first electron transfer, one can expect that E_p would shift by $1.15RT/\alpha F$ for each 10-fold increase in ν. Therefore, the transfer coefficient (α), which is a measure of the symmetry of the energy barrier, can be extracted from a slope of the inset plot of Fig. 4. The obtained α was 0.2, consistent with the literature values (0.15–0.3) [28,29].

Electrochemical reduction of H_2O_2 seems to occur by Eq. (9), which is analogous to the Fenton reaction [30,31]. Immediate decomposition of H_2O_2 would occur after accepting one electron from the electrode,

$$H_2O_2 + e^- \rightarrow {}^{\bullet}OH + OH^- \quad (9)$$

followed by the one-electron reduction of the hydroxyl radical. Imamura et al. verified the presence of hydroxyl radical

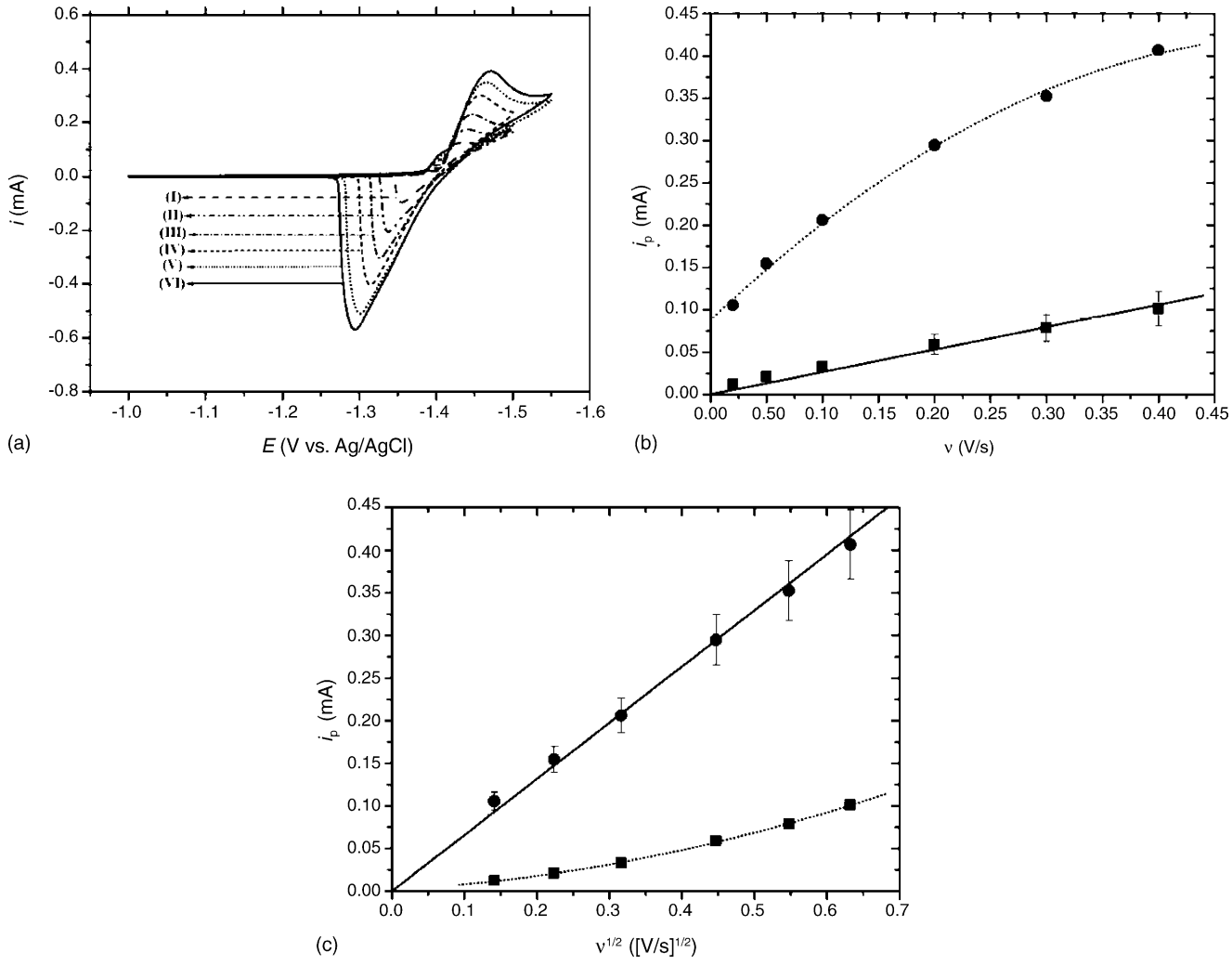

Fig. 2. (a) Cyclic voltammograms (CVs) of 5 mM $Ru(bpy)_3^{2+}$ measured at various scan rates (ν) in pH 7.5 PBS: (I) 0.02 V/s, (II) 0.05 V/s, (III) 0.1 V/s, (IV) 0.2 V/s, (V) 0.3 V/s, and (VI) 0.4 V/s. All CVs were measured at GCE (0.07 cm^2). (b) Dependence of peak current (i_p) on ν. (c) Dependence of i_p on $\nu^{1/2}$. In (b) and (c), squares and circles represent i_p of the first and second waves in CVs shown in (a), respectively. All error bars represent 10% error.

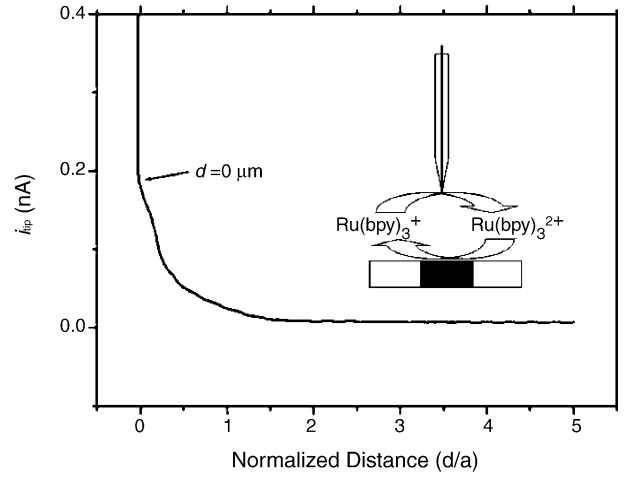

Fig. 3. Experimental approach curve for reduction of 1 mM $Ru(bpy)_3^{2+}$/pH 7.5 PBS in the SG/TC mode. The tip potential was held at −1.2 V and the substrate potential at −1.48 V. Tip approaching rate, 2 μm/s.

(•OH), generated upon electrolysis of H_2O_2, by electron spin resonance (ESR) [32]. The •OH produced has a high redox potential ($E^{\circ\prime}$ = 1.77–1.91 V versus SHE) [33–35] and 99% of initial amount of •OH is usually consumed within 5 μs by reactions with H_2O_2, another •OH, dissolved CO_2 and O_2 [32], and at the electrode.

3.3. Background emission from the $Ru(bpy)_3^{2+}$ solution

Prior to the ECL study, we checked to see if there was any background emission on reduction. For this, pH 7.5 PBS containing 0.1 mM $Ru(bpy)_3^{2+}$ was used and emission was measured in the absence of H_2O_2 by scanning the electrode potential only in a negative direction (0.0 to −2.0 V). As shown in Fig. 5(a) and (b), a small background emission was seen, if the Pt counter electrode was exposed to the solution (Fig. 6(a)). On the other hand, scanning the GCE in a positive direction (0.0 to +1.3 V) did not produce such light. In

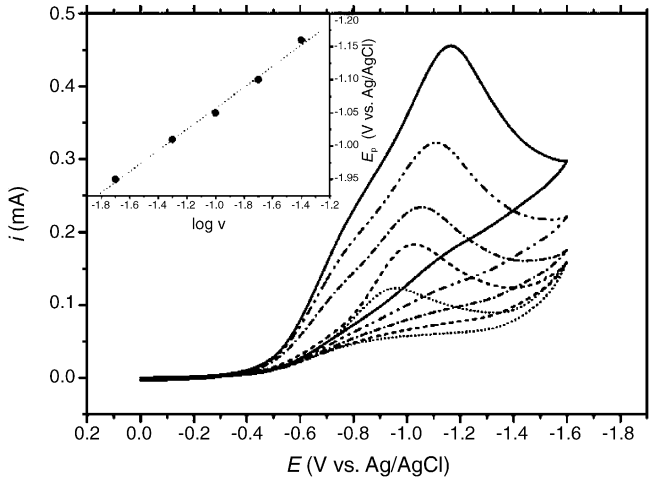

Fig. 4. Cyclic voltammograms (CVs) of 10 mM H_2O_2 in pH 7.5 PBS at different scan rates (bottom to top): 0.02 (···), 0.05 (—, dashed), 0.1 (-·--), 0.2 (-···-), and 0.4 (—, solid) V/s. All CVs were measured at GCE (0.07 cm^2). Inset is a plot of E_p vs. log ν.

the presence of dissolved O_2, this emission occurred when current for O_2 reduction appeared at the working electrode, and continued until the backward potential scan finished (see Fig. 5(a)). After the solution was purged with N_2 for 20 min,

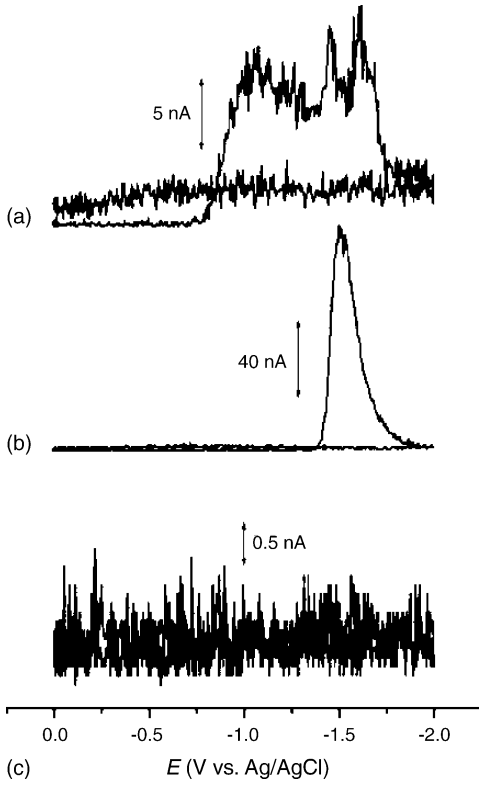

Fig. 5. Plot of background emission vs. *E*. Background emission was measured in pH 7.5 PBS containing only 0.1 mM $Ru(bpy)_3^{2+}$. (a) As-is (no N_2 purging) and exposed counter electrode (Fig. 6(a)), (b) N_2 purging for 20 min and exposed counter electrode (Fig. 6(a)), and (c) N_2 purging for 20 min and an isolated counter electrode (Fig. 6(b)).

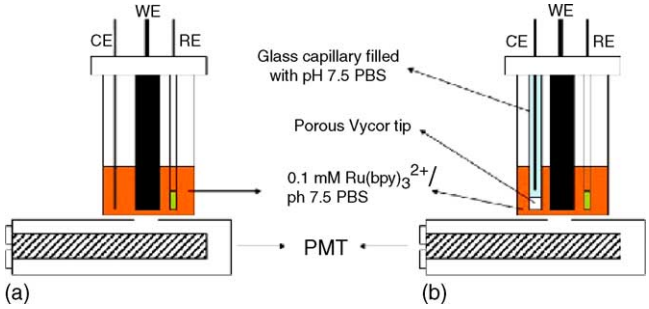

Fig. 6. Electrochemical cells used for ECL measurement. (a) Exposed counter electrode and (b) isolated counter electrode.

the background emission still was observed when current passed for $Ru(bpy)_3^{2+/+}$ (see Fig. 5(b)). This emission had a higher intensity than that measured in the presence of O_2, and also continued until the backward potential scan finished. However, no light emission was observed from 0.0 to −2.0 V (see Fig. 5(c)) when the Pt counter electrode was isolated from the $Ru(bpy)_3^{2+}$-containing solution by a glass capillary and a porous Vycor tip (Fig. 6(b)). The experiments described here bear directly on recent reports by Cao et al. [36] that claimed emission from $Ru(bpy)_3^{2+}$ during the reduction of dissolved oxygen in aqueous solution. According to their emission mechanism, when dissolved O_2 is reduced at the working electrode, reactive oxygen species (ROS), such as H_2O_2, are produced, ultimately leading to hydroxyl radical ($^{\bullet}OH$) which can oxidize $Ru(bpy)_3^{2+}$ to $Ru(bpy)_3^{3+}$. The latter is then reduced to $Ru(bpy)_3^{2+*}$, e.g. by hydroxide ion. Moreover, they reported that addition of TPrA enhanced this cathodic ECL signal. However, our experiments with an isolated counter electrode did not show any emission in a N_2-purged or unpurged solution. In addition, no emission was observed, even in a solution containing 0.1 mM $Ru(bpy)_3^{2+}$ and 100 mM TPrA when an isolated counter electrode was used. Thus, we feel the observation of ECL during a background cathodic scan in our experiments and those in Ref. [36] results from anodic processes at the counter electrode, where the light from that electrode is scattered into the detection device. This suggests that the counter electrode reaction is the main contributor to the background emission, via oxidation of $Ru(bpy)_3^{2+}$. The cell shown in Fig. 6(b) was employed for further ECL studies.

3.4. Reductive-oxidation ECL of $Ru(bpy)_3^{2+}$ with H_2O_2

Fig. 7 shows the simultaneous ECL and CV of 3 mM $Ru(bpy)_3^{2+}$ and 1 mM H_2O_2 in pH 7.5 PBS, measured with a GCE (0.07 cm^2) at 0.1 V/s. When only H_2O_2 was reduced, no luminescence was observed. As the electrode potential approached the potential of $Ru(bpy)_3^{2+}$ reduction, ECL was generated. Its maximum intensity was found at the PL maximum of 620 nm (inset of Fig. 7(b)), demonstrated that $Ru(bpy)_3^{2+*}$ was produced. A suggested ECL mechanism is:

$$H_2O_2 + e^- \rightarrow {}^{\bullet}OH + OH^- \quad (10)$$

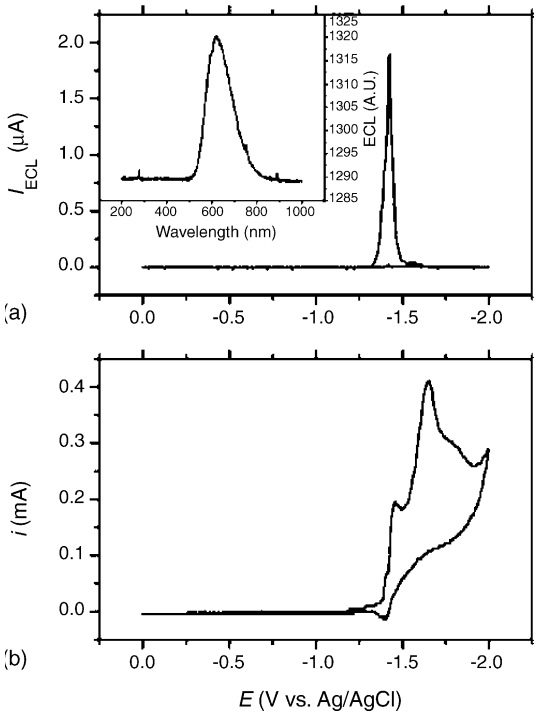

Fig. 7. Simultaneous ECL (a) and CV (b) of 3 mM $Ru(bpy)_3^{2+}$/1 mM H_2O_2 in pH 7.5 PBS. Scan rate = 0.1 V/s. Inset of (a) is the ECL spectrum of this system. GCE (0.07 cm^2) was used for all measurements.

$$Ru(bpy)_3^{2+} + e^- \rightarrow Ru(bpy)_3^{+} \quad (11)$$

$$Ru(bpy)_3^{+} + {}^{\bullet}OH \rightarrow Ru(bpy)_3^{2+*} + OH^- \quad (12)$$

$$Ru(bpy)_3^{2+*} \rightarrow Ru(bpy)_3^{2+} + h\nu \quad (620\,nm) \quad (13)$$

Because of the high redox potential of $^{\bullet}OH$ ($E^{\circ\prime}$ = 1.77–1.91 V versus SHE [33–35]) the produced $^{\bullet}OH$ is a sufficiently strong oxidizing agent to oxidize $Ru(bpy)_3^{+}$ to $Ru(bpy)_3^{2+*}$. To verify this, we estimate the energy ($-\Delta H^{\circ\prime}$) available in Eq. (12) by employing the following equation:

$$-\Delta H^{\circ\prime} \cong E^{\circ\prime}({}^{\bullet}OH/OH^-) - E^{\circ\prime}(Ru(bpy)_3^{2+/+}) - 0.1\,eV \quad (14)$$

where 0.1 eV is an estimate of the entropy term ($T\Delta S^{\circ}$) at 25 °C [1].

Then, $-\Delta H^{\circ\prime}$ was compared with the energy (2.12 eV [12]) of $Ru(bpy)_3^{2+*}$. The estimated $-\Delta H^{\circ\prime}$ was at least 2.95 eV (2.95–3.09 eV), which is higher than the energy of $Ru(bpy)_3^{2+*}$, therefore, Eq. (12) is the energy-sufficient system.

If one considers $E^{\circ\prime}$ of $Ru(bpy)_3^{2+/3+}$ as +1.26 V versus SHE [37], another ECL route is also possible. In addition to Eq. (12), the generated $^{\bullet}OH$ can oxidize $Ru(bpy)_3^{2+}$ to $Ru(bpy)_3^{3+}$. Therefore, annihilation could occur for ECL as follows: Eq. (10) followed by

$$^{\bullet}OH + Ru(bpy)_3^{2+} \rightarrow OH^- + Ru(bpy)_3^{3+} \quad (15)$$

$$Ru(bpy)_3^{3+} + Ru(bpy)_3^{+} \rightarrow Ru(bpy)_3^{2+*} + Ru(bpy)_3^{2+} \quad (16)$$

Although Lytle and Hercules reported light emission by the reaction of $Ru(bpy)_3^{3+}$ and OH^- in strong base [38], this is probably not the ECL mechanism in the present case. The concentration of OH^- produced was buffered in pH 7.5 PBS. This route would also allow the appearance of ECL at H_2O_2 the reduction wave, i.e. $Ru(bpy)_3^{3+}$ formation by reaction with $^{\bullet}OH$ followed by reaction with OH^-, which was not observed.

3.5. Dependence of ECL on $Ru(bpy)_3^{2+}$ and H_2O_2 concentration

To see the effect of the $Ru(bpy)_3^{2+}$ concentration, ECL was measured with a PMT by scanning the electrode potential at 0.1 V/s. Fig. 8 shows a plot of ECL intensity versus $Ru(bpy)_3^{2+}$ concentration. When 1 mM H_2O_2 was used as a reference concentration of coreactant, ECL was not observed at the concentration of $Ru(bpy)_3^{2+}$ less than 0.1 mM. This limitation is probably due to adsorption and precipitation of $Ru(bpy)_3^{+}$. However, ECL was observed from 0.1 mM $Ru(bpy)_3^{2+}$ to 3 mM (Fig. 8). No significant increase in ECL was observed above 3 mM $Ru(bpy)_3^{2+}$ with 1 mm H_2O_2. This may indicate that $^{\bullet}OH$ became the limiting reactant. However, higher concentrations of H_2O_2 caused a decrease in the ECL intensity. Fig. 9 shows how the ECL of 0.1 mM $Ru(bpy)_3^{2+}$ is affected by the H_2O_2 concentration. ECL was measured with a PMT by scanning the electrode potential at 0.1 V/s and the same GCE (0.07 cm^2) was used as in Fig. 8. In this system, ECL was not observed below 5 μM H_2O_2. Weak ECL was detected beginning at 5 μM H_2O_2, and its intensity linearly increased up to 1 mM H_2O_2. At a concentration greater than 1 mM H_2O_2, the ECL intensity exponentially decreased and almost no ECL signal was seen at 90 mM

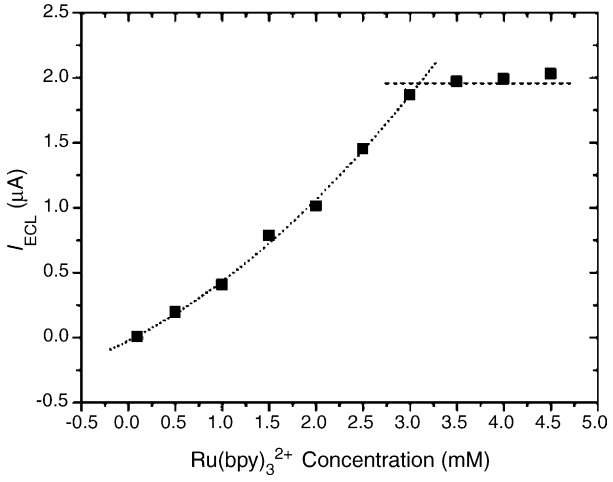

Fig. 8. Dependence of ECL intensity on the concentration of $Ru(bpy)_3^{2+}$, with1 mM H_2O_2 as a reference concentration of coreactant in pH 7.5 PBS. Scan rate 0.1 V/s, GCE (0.07 cm^2).

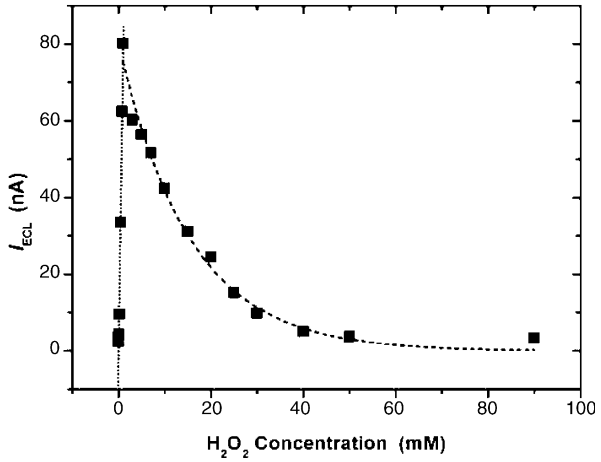

Fig. 9. Dependence of ECL intensity on the concentration of H_2O_2 with 0.1 mM $Ru(bpy)_3^{2+}$ in pH 7.5 PBS. Scan rate 0.1 V/s, GCE (0.07 cm^2).

H_2O_2. This suggests that H_2O_2 can quench the excited state of $Ru(bpy)_3^{2+}$, and this becomes more important at relatively high concentrations.

To test the quenching effect of H_2O_2, photoluminescence (PL) quenching experiments were performed with 2 μM $Ru(bpy)_3^{2+}$ in pH 7.5 PBS. As shown in Fig. 10, PL of $Ru(bpy)_3^{2+}$ was quenched by addition of H_2O_2 without any change in the wavelength of maximum intensity of emission. To quantitatively analyze this quenching, the PL quenching rate constant (k_q) was estimated from the Stern–Volmer relationship (inset of Fig. 10) as defined by [39]:

$$\frac{F_0}{F} = 1 + K_{SV}[H_2O_2] = 1 + k_q\tau[H_2O_2]$$

where F and F_0 denote the PL intensity with H_2O_2 and the initial PL intensity without H_2O_2, respectively, K_{SV} is the Stern–Volmer quenching constant, k_q the PL quenching rate constant, and τ is the lifetime of $Ru(bpy)_3^{2+*}$. The estimated

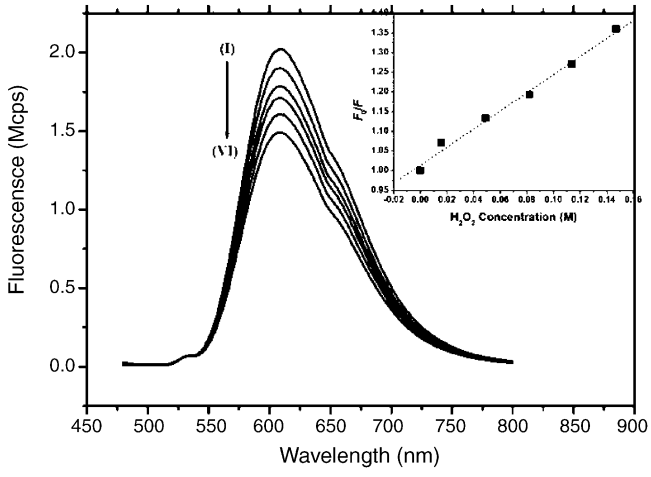

Fig. 10. Photoluminescence (PL) spectra of 2 μM $Ru(bpy)_3^{2+}$ measured with (I) 0 mM, (II) 16 mM, (III) 49 mM, (IV) 82 mM, (V) 114 mM, and (VI) 147 mM of H_2O_2. Inset is the Stern–Volmer plot of PL quenching. A quartz cuvette (1 cm path-length) was used for all measurements.

K_{SV} was 2.3 M^{-1} and k_q was 5.7×10^6 M^{-1} s^{-1} by taking τ as 400 ns [40].

4. Conclusions

Electrochemical reduction of $Ru(bpy)_3^{2+}$ in an aqueous solution induces three different forms of $Ru(bpy)_3^{+}$: (1) adsorbed, (2) precipitated, and (3) dissolved. Because it produces $^{\bullet}OH$, H_2O_2 can be used as a coreactant for reductive-oxidation ECL. In the $Ru(bpy)_3^{2+}/H_2O_2$ system, ECL is generated mainly by high energy ET between dissolved $Ru(bpy)_3^{+}$ and $^{\bullet}OH$. Excess H_2O_2 quenches both ECL and PL. While oxidative-reduction ECL of $Ru(bpy)_3^{2+}$ is detected as low as ~pM in an aqueous solution containing oxalate or TPrA [13], the limit of reductive-oxidation ECL of $Ru(bpy)_3^{2+}$ is about 100 μM probably due to adsorption and precipitation of $Ru(bpy)_3^{+}$.

Acknowledgements

Support from the Texas Advanced Research Program (0103) and Igen, Inc., is gratefully acknowledged. JPC thanks Dr. Janine Mauzeroll for fabrication of the carbon fiber tip.

References

[1] L.R. Faulkner, A.J. Bard, in: A.J. Bard (Ed.), Electroanalytical Chemistry, vol. 10, Marcel Dekker, New York, 1977, p. 1.
[2] A.J. Bard, J.D. Debad, J.K. Leland, G.B. Sigal, J.L. Wilbur, J.N. Wohlstadter, in: R.A. Meyer (Ed.), Encyclopedia of Analytical Chemistry: Applications, Theory, and Instrumentation, Wiley, New York, 2000, p. 9842.
[3] A.J. Bard (Ed.), Electrogenerated Chemiluminescence, Marcel Dekker, New York, 2004.
[4] M.-M. Chang, T. Saji, A.J. Bard, J. Am. Chem. Soc. 99 (1977) 5399.
[5] I. Rubinstein, A.J. Bard, J. Am. Chem. Soc. 103 (1981) 512.
[6] J.B. Noffsinger, N.D. Danielson, Anal. Chem. 59 (1987) 865.
[7] J.K. Leland, M.J. Powell, J. Electrochem. Soc. 137 (1990) 3127.
[8] Y. Zu, A.J. Bard, Anal. Chem. 72 (2000) 3223.
[9] F. Kanoufi, Y. Zu, A.J. Bard, J. Phys. Chem. B 105 (2001) 210.
[10] H.S. White, A.J. Bard, J. Am. Chem. Soc. 104 (1982) 6891.
[11] W.G. Becker, H.S. Seung, A.J. Bard, J. Electroanal. Chem. 167 (1984) 127.
[12] E.F. Fabrizio, I. Prieto, A.J. Bard, J. Am. Chem. Soc. 122 (2000) 4996.
[13] W. Miao, J.-P. Choi, A.J. Bard, J. Am. Chem. Soc. 124 (2002) 14478.
[14] A.-M. Andersson, R.H. Schmehl, Mol. Supramol. Photochem. 7 (2001) 153.
[15] A.W. Knight, in: A.M. Grarcia-Campana, W.R.G. Baeyens (Eds.), Chemiluminescence in Analytical Chemistry, Marcel Dekker, New York, 2001, p. 211.
[16] M.M. Richter, in: F.S. Ligler, C.A.R. Taitt (Eds.), Optical Biosensors: Present and Future, Elsevier, New York, 2002, p. 173.
[17] A.W. Knight, Trends Anal. Chem. 18 (1999) 47.
[18] G.D. Christian, W.C. Purdy, J. Electroanal. Chem. 3 (1962) 363.
[19] A.J. Bard, F.-R.F. Fan, J. Kwak, O. Lev, Anal. Chem. 61 (1989) 1794.
[20] P. McCord, A.J. Bard, J. Electroanal. Chem. 318 (1991) 91.

[21] G.C. Fiaccabrino, M. Koudelka-Hep, Y.-T. Hsueh, S.D. Collins, R.L. Smith, Anal. Chem. 70 (1998) 4157.
[22] N.E. Tokel, A.J. Bard, J. Am. Chem. Soc. 94 (1972) 2862.
[23] N.E. Tokel-Takvoryan, R.E. Hemingway, A.J. Bard, J. Am. Chem. Soc. 95 (1973) 6582.
[24] R.H. Wopschall, I. Shain, Anal. Chem. 39 (1967) 1514.
[25] A.J. Bard, L.R. Faulkner, Electrochemical Methods, 2nd ed., Wiley, New York, 2001, Chapter 14.
[26] H.S. White, A.J. Bard, J. Am. Chem. Soc. 104 (1982) 6891.
[27] A.J. Bard, in: M.V. Bard, Mirkin (Eds.), Scanning Electrochemical Microscope, Marcel Dekker, New York, 2001, Chapter 1.
[28] O. Hammerich, in: A.J. Bard, H. Lund (Eds.), Encyclopedia of Electrochemistry of the Elements, Marcel Dekker, New York, 1978, p. 316.
[29] M.F. Romantsev, É.S. Levin, J. Anal. Chem. USSR 18 (1963) 957.
[30] H.J.H. Fenton, J. Chem. Soc. 65 (1894) 899.
[31] C. Walling, Acc. Chem. Res. 8 (1975) 125.
[32] K. Imamura, Y. Tada, H. Tanaka, T. Sakiyama, K. Nakanishi, J. Colloid Interf. Sci. 250 (2002) 409.
[33] W.H. Koppenol, J.F. Liebman, J. Phys. Chem. 88 (1984) 99.
[34] H.A. Schwarz, R.W. Dodson, J. Phys. Chem. 88 (1984) 3643.
[35] U.K. Kläning, K. Sehested, J. Holcman, J. Phys. Chem. 89 (1985) 760.
[36] W. Cao, G. Xu, Z. Zhang, S. Dong, Chem. Commun. (2002) 1540.
[37] K. Kalyanasundaram, Coord. Chem. Rev. 46 (1982) 159.
[38] F.E. Lytle, D.M. Hercules, J. Am. Chem. Soc. 88 (1966) 4745.
[39] F. Wilkinson, in: G.G. Guilbault (Ed.), Fluorescence: Theory, Instrumentation, and Practice, Marcel Dekker, New York, 1967, Chapter 1.
[40] R. Ballardini, M.T. Gandolfi, V. Balzani, Inorg. Chem. 26 (1987) 862.